



PERGAMON

Neural Networks 15 (2002) 635–645

Neural
Networks

www.elsevier.com/locate/neunet

2002 Special issue

Neuromodulation of decision and response selection

Marius Usher^{*,1}, Eddy J. Davelaar

School of Psychology, Birkbeck College, University of London, Malet Street, London WC1E 7HX, UK

Received 24 October 2001; accepted 19 April 2002

Abstract

We present a model for the attentional neuromodulation of decision and selection processes. The model assumes that phasic responses in the brain nucleus Locus Coeruleus modulate, via the transmission of norepinephrine, the synaptic efficiency of neural circuits, at specific (stimulus and task dependent) time intervals. The model is applied first, to a task of perceptual choice, simulating attentional fluctuations and accounting for a series of behavioral and neurophysiological data. Second, the flexibility of information processing, whereby the parameters of the local circuits are modified online, is illustrated in the application of the model to a task of selection from short-term memory. © 2002 Published by Elsevier Science Ltd.

Keywords: Attention; Neuromodulation; Locus Coeruleus; Norepinephrine; Selection; Response-time

1. Introduction

Neuromodulators such as norepinephrine (NE) and dopamine are often assumed to mediate the attentional control of cognitive processing (Arnsten, 1998; Cohen & Servan-Schreiber, 1992). In a previous article (Usher, Cohen, Servan-Schreiber, Rajkowski, & Aston-Jones, 1999) we have presented neurophysiological and behavioral data (see also Aston-Jones, Rajkowski, Kubiak, & Alexinsky (1994)) showing that changes in NE responses of the brain nucleus Locus Coeruleus (LC) correlate with behavioral responses in awake monkey and we presented a neurocomputational model addressing the attentional mechanism of NE neuromodulation. In this paper, we extend and develop this computational model for NE neuromodulation to a wider domain of cognitive tasks that require decision and response selection. The first domain corresponds to perceptual choice situations, being a direct extension of the LC model presented in Usher et al. (1999). To do this we review data on attentional phases of LC responses in the LC, and show how a simplified model for LC response, functionally similar with the one derived by Gilzenrat, Holmes, Rajkowski, Aston-Jones, and Cohen (2002), can account for a variety of behavioral findings and leads to novel

predictions. The second domain corresponds to a more complex cognitive process that involves memory maintenance followed by a probe-triggered response selection.

2. Attentional control and LC responses in perceptual choice

Previous behavioral studies of LC neuromodulation involved a simple go–nogo task (Aston-Jones et al., 1994). In this task monkeys are presented with a long sequence of stimuli, one type of which is designated as a ‘target’ that requires a lever-release, while all the other types are designated as ‘nontargets’ (or distractors) requiring to withhold responses. Typically, the target has a low frequency and the monkey needs to maintain vigilance in order to respond as fast as possible to targets without producing false alarms (FA—responses to nontargets). After training, the monkeys perform the task at a high level of accuracy. Nevertheless, during long behavioral intervals, significant fluctuations in the level of performance occur spontaneously in a remarkable correlation with the response pattern of the LC neurons (Usher et al., 1999). During ‘good’ behavioral periods when the number of FAs is low, the spontaneous level of LC (tonic) response is also low but the evoked (phasic) responses, specific to targets, are peaked and pronounced. In

* Corresponding author. Tel.: +44-207-631-6312; fax: +44-207-631-6201.

E-mail address: m.usher@bbk.ac.uk (M. Usher).

¹ www.psyc.bbk.ac.uk/staff/mu.html

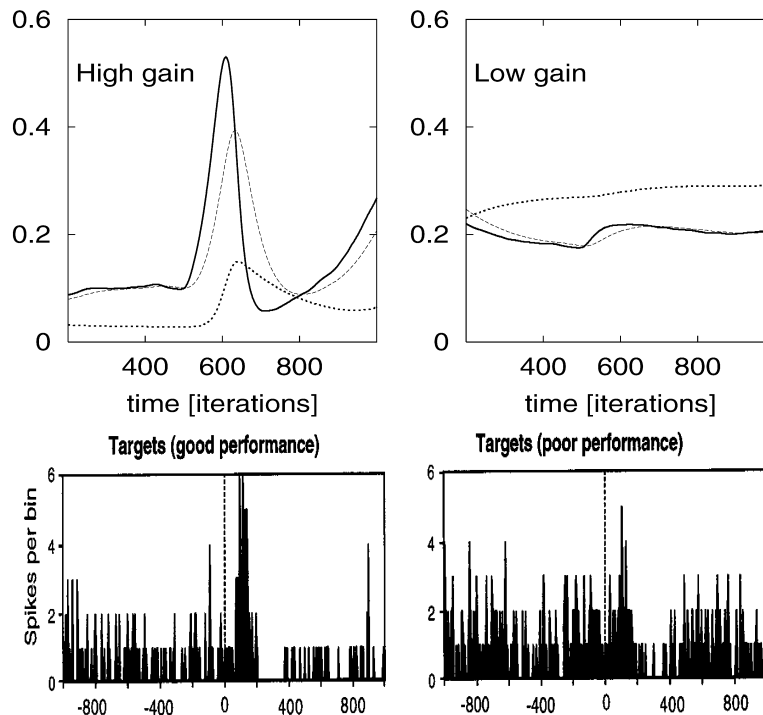


Fig. 1. Top: LC response (x -unit) for the x -unit (bold solid line), the y unit (dotted bold line) and the NE-response (thin dashed line) for high and low gain values, in response to an input (of 0.2) applied at $t = 500$. Bottom: responses in the LC to targets during good (left) and poor (right) behavioral intervals. (From Usher et al. (1999), *Science*, 283, 549–554. Permission pending.)

contrast, during ‘poor’ behavioral periods when the level of FAs is relatively high, the tonic LC response is higher while the phasic response to targets is reduced (Fig. 1, bottom). Importantly, the reduction in the level of FA is not due to a speed-accuracy tradeoff, as it is not accompanied by an increase in response time (RT). Nevertheless, a very specific pattern of RT distribution distinguishes responses in good versus poor behavioral intervals. While the two distributions have similar mean RT, the distribution of responses during the good behavioral periods is narrower as shown in Fig. 4 (top). In our previous model, these changes in the level of performance and in LC response patterns were explained as resulting from variations in the coupling of the LC neurons via gap-junctions (Usher et al., 1999). The model for the LC used in that work was based on a complex integrate-and-fire model with 250 units with electrotonic coupling as well as chemical interactions with different time scales. Although the model was able to explain all the behavioral and LC response patterns with a change of a single parameter—the electrotonic coupling—its complexity affects the transparency of the explanation. Here we develop a simplified model for the LC neuromodulation, which inherits most of the response properties of the original model (see also Gilzenrat et al. (2002)) and we show how it can be used to account for the effects of attentional neuromodulation in a wider set of cognitive tasks.

3. A ‘functional’ model for LC modulation

3.1. Model

The functional LC model described in this section is embedded in a behavioral model for perceptual choice and for selection from memory. Since the same LC model is used in both of these tasks, we first describe its mechanism and its attentional modes that are designed to account for the neurophysiological data in the LC described earlier.

The functional model for the LC is not attempted to be neurophysiologically realistic but only to provide an equivalent functional behavior to that found in the data and captured in our previous LC model (Usher et al., 1999). A formal reduction of that model to an effective nonlinear system with two variables is presented by Gilzenrat et al. (2002), on the basis of the FitzHugh–Nagumo oscillator. The simplified model of the LC we use here is based on another nonlinear system with two variables: the Wilson–Cowan (excitatory–inhibitory) population system (Wilson & Cowan, 1972). The model is, however, functionally equivalent to the formally reduced model (see Gilzenrat et al., 2002 in their Appendix).

The main features that the functional model was required to satisfy are: (i) phasic responses to target stimuli with a low tonic baseline, (ii) a parameter that corresponds to attentional modulation (or to the gap-junction coupling in our previous model) that controls these attentional modulations, (iii) for a value of the parameter that corresponds to high alertness, the

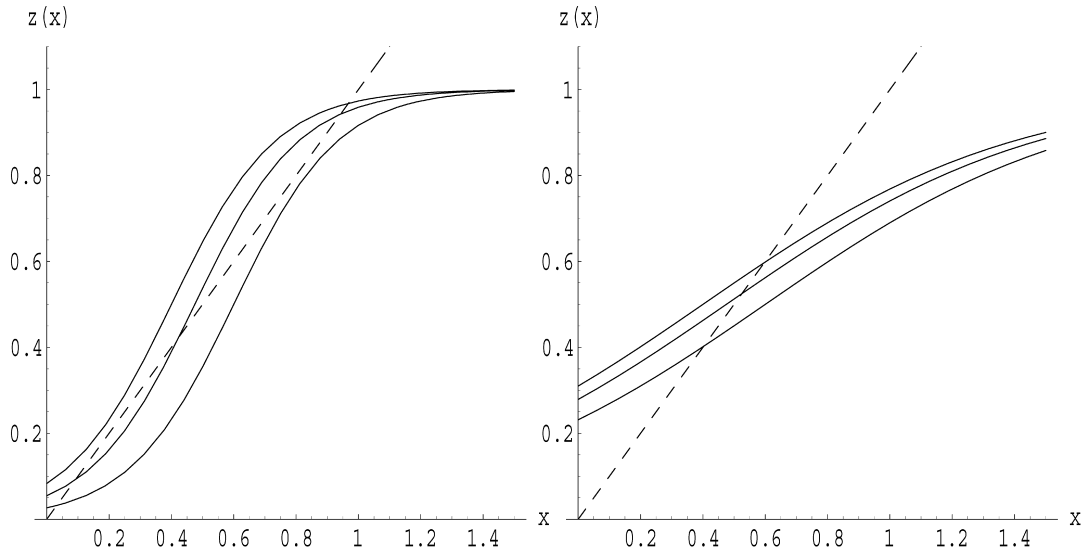


Fig. 2. The steady state solutions for the x -dynamics are intersections of the $z = F(g, x, I_x, y)$ curve (solid lines) with the identity map, $z = x$ (dashed). Left: high gain, $g = 3$ and Right: low gain, $g = 1$. The three solid lines correspond to small changes in the input, $I_x : 0.45, 0.3, 0.05$.

phasic response should be pronounced and the baseline reduced and (iv) for a value of the parameter corresponding to low alertness, the phasic response is reduced while the baseline increases (Fig. 1, bottom).

The model, satisfying these requirements, is given by the following equations that characterize its dynamics in discrete time steps (see Section 3.3 for the differential form of the equations):

$$\begin{aligned} x(t+1) &= \lambda_x x(t) + (1 - \lambda_x) F[g(a_x x(t) - by(t) + I_x(t) - \theta_x)], \\ y(t+1) &= \lambda_y y(t) + (1 - \lambda_y) F[g(a_y x(t) - \theta_y)] \end{aligned} \quad (1)$$

where F is the logistic sigmoidal function $F(x) = 1/(1 + \exp(-x))$. The x and y variables correspond to excitatory/inhibitory populations,² with decay parameters λ_x and λ_y ($\lambda_y \gg \lambda_x$) and with thresholds θ_x and θ_y , respectively. Among these variables, x reflects to the instantaneous LC activation, which we compare with that found in neurophysiological recordings, while y is only an auxiliary variable. The output of the system, is the NE released by the LC which is computed from the LC-activation, x : $NE(t+1) = \lambda_{NE} NE(t) + (1 - \lambda_{NE}) x(t)$. NE is thus a delayed and integrated measure (with exponential decay) of the instantaneous LC activation, $x(t)$ and I_x is the input to the LC. The main parameter that affects attentional manipulation, is the gain of the sigmoidal function, g .

3.2. Results

In the following, the LC model was presented with input (corresponding to a target in the perceptual choice task used

² Those variables do not correspond to excitatory/inhibitory populations in the LC but are abstract variables that capture the functional behavior of the system.

in the experiment) at $t = 500$ iterations of the computer simulation (I_x is increased by 0.2) and the response of the LC model is reported for two levels of the gain-parameter, g , that controls the slope of the logistic function, F . The two values of gain used here are: $g = 1$ for low gain and $g = 3$ for high gain. The other parameters, which were kept constant in all the simulations, are reported in Appendix A. The LC responses, $x(t)$, $y(t)$, and the output $NE(t)$ for these two cases are shown in Fig. 1 (top).

One can observe that higher g -values results in pronounced phasic responses and reduced baseline, while low g -values in high baseline with reduced phasic responses, reflecting the pattern found in the experimental data for high/low attentional modes. In the following we will relate to these two attentional modes as: the phasic mode (high-gain) and the tonic mode (low-gain).

3.3. Discussion

The key to understand the behavior of this system is to distinguish between the ‘fast’ variable x ($\tau_x = 1/(1 - \lambda_x) = 14$) and the much slower variable y ($\tau_y = 1/(1 - \lambda_y) = 200$). This allows the use of an *adiabatic* approximation, where one solves first the one-dimensional dynamics of the x variable (assuming a constant y) towards its equilibrium x^* . Using the differential form of the iterative equations, Eq. (1) (see also Gilzenrat et al. (2002) or Usher & McClelland (2001)) this can be formulated as:

$$\frac{dx}{dt} = -x + F[g(ax - by + I_x - \theta_x)] = 0 \quad (2)$$

After determining the stable solution of this equation, $x^*(y)$, one examines how the equilibrium, x^* , depends on the slow variable, y , whose equilibrium point is monotonic in the value of x^* [$y^* = F(a_y x^* - \theta_y)$]. This qualitative analysis is

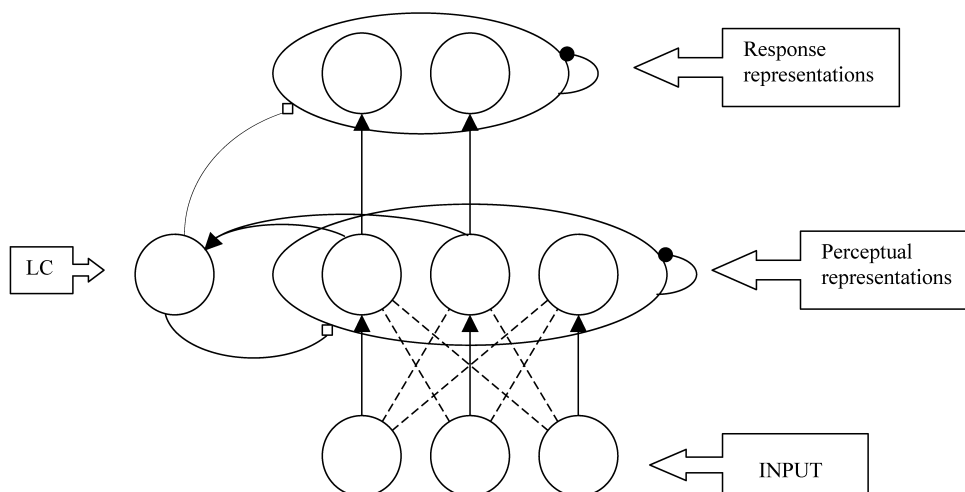


Fig. 3. Scheme of the computational model. Solid arrows correspond to excitatory links, solid circles to lateral inhibition and open squares to neuromodulation.

shown in Fig. 2 for high gain (left panel) and for low gain (right panel), where three solutions are shown corresponding to the combined value of $I_x - by$. The middle solid curves are obtained for $I_x - by = 0.3$ and correspond to the stationary state before the application of the input ($t = 500$ in Fig. 1, where y is close to zero).

One can observe, that while the high gain system is bistable [it has two stable solutions—the extreme intersections between the identity line ($z = x$; dotted) and the $z = F(x)$ curve (solid middle line)—the lower one being consistent with the y -equation] the low gain system has a single stable solution. A relatively small increase in the input to the LC, $I_x = 0.45$, moves the $z = F(x)$ curve to the left. Since this destroys the lower solution, the systems shoots towards the upper solution, corresponding to the phasic LC response in Fig. 1 (left panel). This leads to a slower increase in y that modifies the input $I_x - by$ to the lower value of 0.05 and sends the x -variable to a new steady state solution at low x , corresponding to the termination of the phasic response. This scenario, does not occur for low gain, where small changes in input lead only to correspondingly small changes in the steady state values of x (reduced phasic response, in Fig. 1, right panel). A more rigorous analysis of this system as well as of the FitzHugh–Nagumo one, based on two-dimensional phase-plane techniques in presented by Gilzenrat et al. (2002) in their Appendix.

4. Behavioral model for the perceptual task

In this section, the model is applied to a straightforward extension of the go/nogo task described earlier—a forced choice between two response alternatives, both targets that require a response and which need to be distinguished from distractors that require the withholding of response (e.g. ‘respond to digits: 1 vs. 2 with the corresponding button and ignore letters’). The computational model used to address this task is shown in Fig. 3. It includes an input layer, a layer

of perceptual representations (for both the targets and the distractors) and a layer of response representations (only for the two targets) corresponding to motor responses. The LC, which is modeled as described earlier, receives input from the two perceptual target representations (these links are assumed to be learned during practice with the task), $I_x(t) = \sum_{i=1,2} f_i$, and projects neuromodulation, $NE(t)$, to all the units in the perceptual and response representations.

4.1. Neural dynamics and activation functions

The equations used for the dynamics of the neural activation, x , in the system, follow a stochastic version (Usher & McClelland, 2001) of the classical cascade (McClelland, 1979) and Brain-State-in-a-Box (Anderson, Silverstein, Ritz, & Jones, 1977) equations:

$$x(t+1) = \lambda x(t) + (1 - \lambda)I(t) \quad (3)$$

where $\lambda < 1$ is a neural decay coefficient, which is related to the decay time constant, τ , ($\lambda = 1 - 1/\tau$) of the corresponding differential equation $dx/dt = -(x/\tau) + I$. From a neurophysiological perspective, the activation corresponds to a dynamical input current that is subject to exponential decay (Abbott, 1992; Amit & Tsodyks, 1991). The output (or firing rate), f , is related to the input (or activation) by a sigmoidal activation function, $f = G(x)$. The activation function we use here is given by:

$$G(x) = 0, \quad \text{for } x < 0$$

$$G(x) = \frac{x}{1+x}, \quad \text{for } x > 0 \quad (4)$$

The response function G is similar to the threshold linear function (Anderson et al., 1977; Usher & McClelland, 2001) with the addition of a saturation nonlinearity: $x/(1+x)$. As discussed in Usher and McClelland (2001), the threshold nonlinearity is important for preventing negative activations (that have no biological reality but could appear in a linear system due to noise and lateral inhibition) from producing a

spurious enhancing of activation when multiplied by inhibitory weights. Logistic activation functions also bound the activation to the positive range, but as discussed in Usher and McClelland (2001), threshold-linear activation functions produce better fits to the neurophysiological recordings at low firing rates than the more often used logistic functions (Ahmed, Anderson, Douglas, Martin, & Nelson, 1995; Ahmed, Anderson, Douglas, Martin, & Whitteridge, 1998; Jagadeesh, Gray, & Frester, 1992; Mason & Larkman, 1990). The nonlinearity used here, has the advantage of being close to linear for small input ($x < 1$) and of showing a gradual saturation towards a maximum activation level of one (corresponding to maximal firing rate) at large input ($x > 1$). In previous work, this activation function was shown to be useful in modeling the maintenance of neural activation in the pre-frontal working-memory (WM) system (Davelaar & Usher, 2002; Haarmann & Usher, 2001; Usher & Cohen, 1999; see also O'Reilly & Munakata (2000), pp. 46–49 for a more detailed textbook explanation of this activation function (labelled XX1)).

4.2. The network

4.2.1. Perceptual units

The perceptual units are clamped at the stimulus onset with values that depend on the stimulus shown. Here we used a simplified localistic scheme that takes feature overlap between representations into account. When a stimulus is present, its input is clamped to $I = 0.45$ while the input of the other two units are clamped to $I = 0.275$ (sum of the inputs is normalized to unity). During the interval before input is presented, a background input, $I_0 = 0.2$ is assumed for all units.

The dynamic equations for the perceptual units are given below in terms of discrete time step iterations:

$$p_i(t + 1) = \lambda p_i(t) + (w^0 - \lambda) \times \left[(1 + cNE(t))I_i(t) + (\alpha_p + cNE(t))G(p_i(t)) - (\beta_p + cNE(t)) \sum_{j \neq i} G(p_j(t)) + noise \right] \quad (5)$$

where p_i is the unit activation, $\lambda < 1$ is a decay constant for neural activity, w^0 (which is set to unity, $w^0 = 1$) is a feedforward synaptic projection to the perceptual layer and the coefficients α and β correspond to recurrent excitation and lateral inhibition, respectively (Usher & McClelland, 2001).

The variable NE(t) corresponds to the neuromodulation contributed by the LC, which we assume to increase the magnitude of both the excitatory and the inhibitory weights (Cheun & Yeh, 1992; Devilbiss & Waterhouse, 2000; Sessler et al., 1995; Waterhouse, Mouradian, Sessler, & Lin, 2000) in proportion with the NE level and c is a neuromodulation

Table 1

	Gain	1.0		3.0	
		%	RT(SD)	%	RT(SD)
Target	Correct response	97.6	89(37)	99.2	91(24)
	Incorrect response	2.4	28(24)	0.8	52(38)
Distractor	False alarms	20.7	160(118)	9.4	188(112)
	Correct rejections	79.3	–	90.6	–

coefficient. Finally, zero mean Gaussian noise, with standard deviation, σ_p , σ_r (for perceptual/response units), is independently added to each unit at each time iteration.

4.2.2. Response units

The dynamic equations for the response units follow similar equations

$$r_i(t + 1) = \lambda r_i(t) + (1 - \lambda) \times \left[(W^{rp} + cNE(t))G(p_i(t)) + (\alpha_r + cNE(t))G(r_i(t)) - (\beta_r + cNE(t)) \sum_{j \neq i} G(r_j(t)) + noise \right] \quad (6)$$

Here the output of the perceptual units $G(p_i)$ multiplied by a

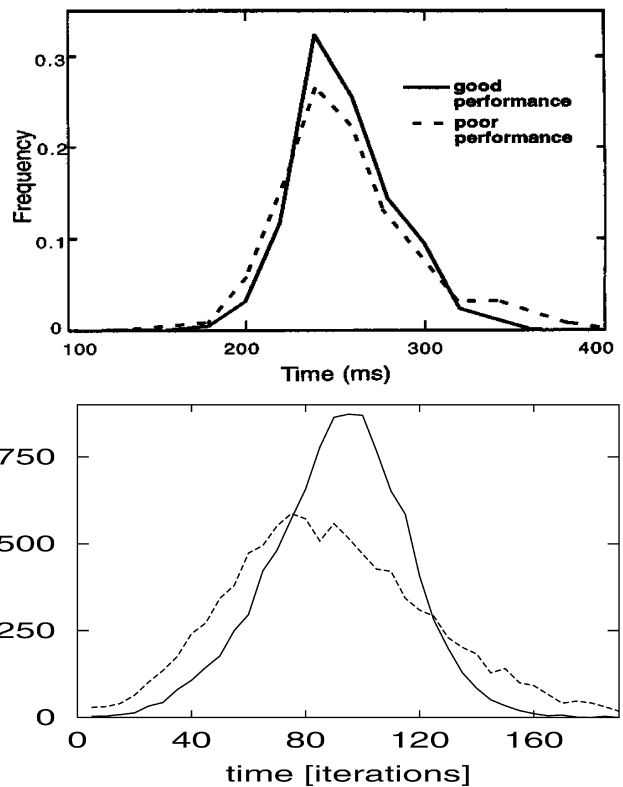


Fig. 4. Top: RT distributions to targets during good/poor behavioral intervals (From Usher et al. (1999), Science, 283, 549–554. Permission pending. Bottom: RT distributions for correct responses in the model with high gain, $g = 3$ (solid) and with low gain, $g = 1$ (dashed).

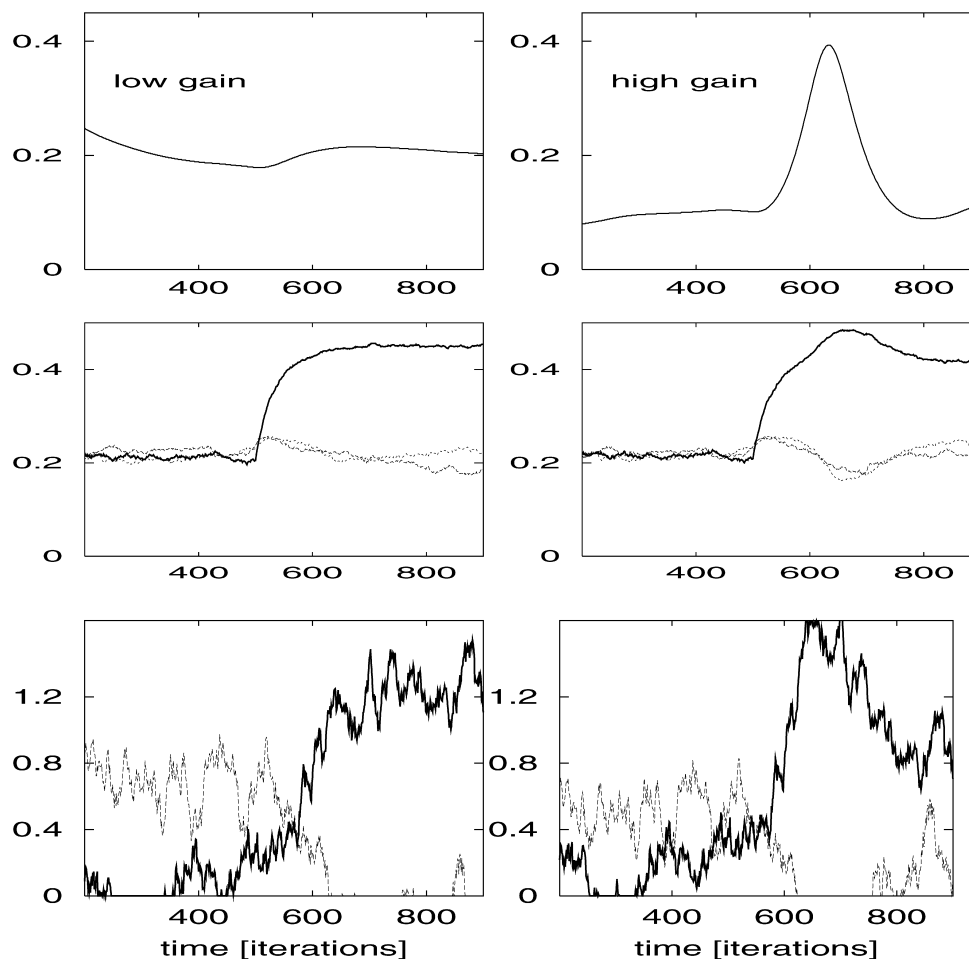


Fig. 5. Top: NE responses in the computer simulation of the perceptual choice task. Middle: firing rate ($G(p_i)$) responses of perceptual units; Bottom: firing rate ($G(r_i)$) of response units, for low gain (left) and high gain (right). The stimulus is presented at $t = 500$ iterations.

synaptic weight, W^p , provides the input and a separate set of excitation/inhibition parameters α_r and β_r is used. A response is generated when the first response unit reaches an activation criterion (Usher & McClelland, 2001), z , which is fixed to the value of $z = 1$.

4.3. Results

Examples of the LC responses for high/low levels of gain in a single trial of this simulation were shown in Fig. 1. In order to examine the behavioral patterns, sets of 10 000 simulation trials were run for target and for distractor stimuli at the two levels of gain. The results are presented in Table 1, with regards to accuracy (percent correct responses, incorrect responses and FAs) and RTs. As we only attempt to obtain a qualitative explanation of the data patterns, the RTs are reported in 'steps of the computer simulation' (or iterations).

We observe that increasing the gain leads to a significant decrease in FAs and a slight increase in the fraction of correct responses (this fraction is already close to ceiling, however, as is to be expected for a perceptual choice with

clearly distinguishable stimuli; this is also found in data of the go-nogo task where the hit rate is close to ceiling (Usher et al., 1999)).

The RT distribution for high gain is narrower than for the low gain, (Fig. 4), while the mean RTs are equivalent. This pattern reflects the RT distributions in the experimental data, for intervals with high and low phasic responses.

4.4. Discussion

The NE response and the activations of the perceptual and response units for a single trial (with a target stimulus presented at $t = 500$ iterations) for low and high gain levels are shown in Fig. 5.

We observe that at stimulus presentation, $t = 500$, there is an increase in the activation of all three perceptual units (the two targets and the distractor). The correct response unit receives stronger input and inhibits the activations of the incorrect target and distractor unit. This residual response, however, can help the pre-stimulus noise activation of the response units to generate an incorrect choice (the incorrect unit reaching the response criterion

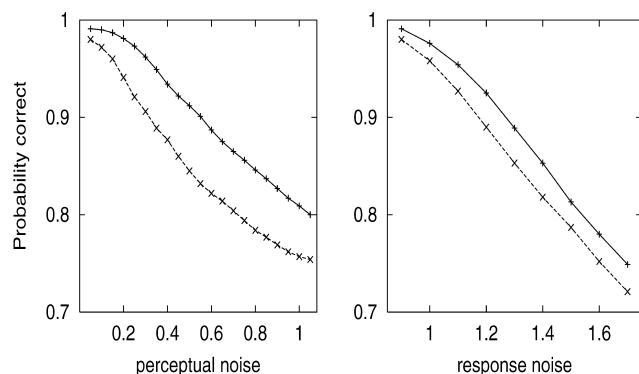


Fig. 6. The effect of perceptual and response noise on the accuracy of choice in the model for high (solid) and for low (dashed) gains.

before the correct one; this happens in only 2.4% of trials). Increasing the gain (right) has two major effects on the activations. First, the lower tonic activation of the LC unit reduces the noise activation of the response units in the pre-stimulus interval, leading to a reduction in anticipatory or incorrect responses (including FAs). Second, the pronounced phasic response, amplifies the activations of all the units (due to amplification of synaptic input, including the input) and it also amplifies the amount of competition (which is affected by both the recurrent excitation and the lateral inhibition parameters) between the representation units. With high gain, one can observe that, following the transients; the activation of the incorrect units is strongly suppressed. This complex pattern of phasic neuromodulation has the effect of reducing the error rate and the rate of FAs without a sacrifice in RT. The phasic neuromodulation enhances processing and narrows it down around the stimulus presentation, explaining the reduction in the tails of the RT distribution.

The computer simulations, described earlier were done with parameters that provide a high level of performance in the choice of targets (less than 3% errors) even in the nonphasic mode. This corresponds to an easy type of discrimination as was the case in the experimental studies of neuromodulation we address here (Aston-Jones et al., 1994). In order to explore the effect of the phasic mode on a wider range of performance levels, we conducted a different set of simulations where we increase the level of noise over the perceptual and over the response units. The comparison between the high- g and the low- g neuromodulation modes on performance is shown in Fig. 6. As the noise level increases, the choice accuracy decreases as expected. Importantly, the advantage of high-gain modulation on task performance is maintained at all levels of noise.

5. Response selection and memory maintenance

The cognitive task described earlier can be fully characterized as a choice of one out of many alternatives.

In a recent work (Usher & McClelland, 2001) we have proposed that lateral inhibition between competing representations is a powerful mechanism suited to perform this type of winner-take-all selection. There are other cognitive tasks, however, where a winner-take-all selection is not advantageous. A simple example for such situations is a short-term memory (STM) test, where participants are presented with a sequence of items (say words) that have to be maintained in order to answer a memory probe test presented later on. Assume, for example, that following a sequence of four words (each chosen from a distinct semantic category), a cue corresponding to one of the four categories is presented and participants are required to produce the word that belongs to that category from the current trial (see, e.g. Exp. 2 in Haarmann and Usher (2001)). Although the task requires a winner-take-all selection, this selection needs to be delayed until the cue appears. Before this event, a system with a moderate level of inhibition that can maintain few items in active memory (Cowan, 2001; Haarmann & Usher, 2001; Usher & Cohen, 1999; Usher, Cohen, Haarmann, & Horn, 2001) can be of better use. At cue presentation, however, the task demand changes from a memory maintenance to one of selection. A flexible cognitive system needs, not only to be able to perform each of these tasks separately, but to perform them together in a synergistic way. Here we show that the mechanism of neuromodulation offers a simple way to achieve such flexibility, by enabling the online modification in the values of network parameters, such as lateral inhibition and recurrent excitation, in relation to task demands.

5.1. Modeling semantic cued recall in STM

To model the situation described earlier, we use a model with the same type of architecture as the one described in Section 4. The scheme for this model is shown in Fig. 7.

Here, the middle representation corresponds to a WM system assumed to reside in the pre-frontal cortex (Usher & Cohen, 1999) and to mediate the activity found in delayed match to sample tasks in this cortical area (Goldman-Rakic, 1992; Miller, Erickson, & Desimone, 1996). The units of representation in this module have a high value of recurrent excitation ($\alpha = 1.9$) that enables the maintenance of activations after stimulus offset and they compete via lateral inhibition (as in Section 4).

$$x_i(t+1) = \lambda x_i(t) + (1 - \lambda)$$

$$\times \left[\alpha G(x_i(t)) - \beta \sum_{j \neq i} G(x_j(t)) + I_i(t) \right] \quad (7)$$

5.1.1. Active maintenance and capacity

In a previous work (Usher & Cohen, 1999) we showed that when the recurrent excitation parameter is larger than unity ($\alpha > 1$), the capacity can be easily derived, when the

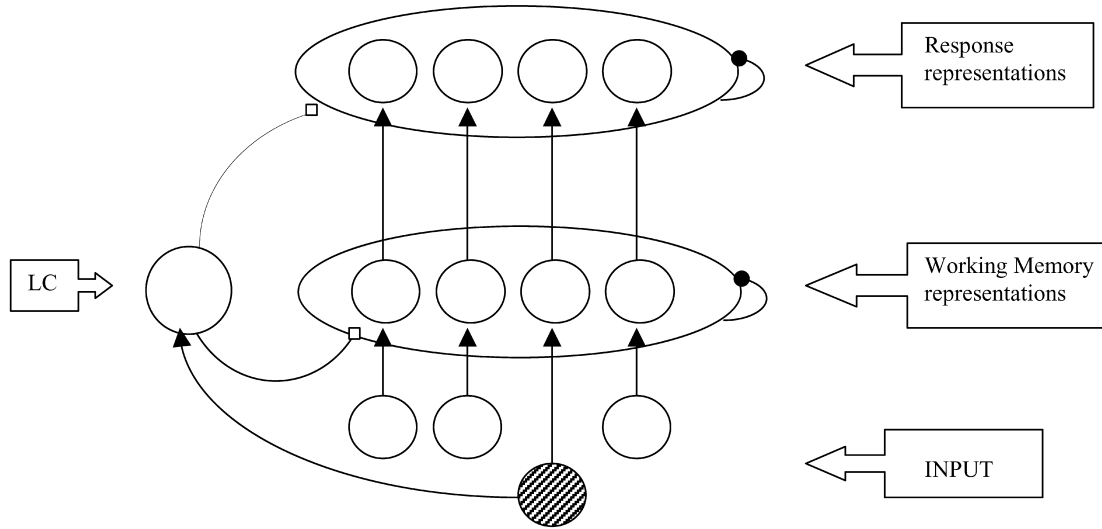


Fig. 7. Scheme of the computational model. Solid arrows correspond to excitatory links, solid circles to lateral inhibition and open squares to neuromodulation.

activation function is given by Eq. (4). Two properties of this system may be important to review here. First, as more items, n , are maintained in active state without input, their activation decreases as: $x(n) = \alpha - 1 - \beta(n - 1)$. Thus the activation of an n -state solution decreases linearly with n . Second, when the number of activated units exceeds a boundary (that depends on α and β , the solution $x(n)$ loses its stability and as a result one of the units is deactivated.³ These two properties of the system are shown in Fig. 8.

The system has thus a limited capacity, consistent with experimental findings in human short term memory (Cowan, 2001). In our present model, the WM representations compete via lateral inhibition which is set at a value $\beta = 0.2$. This creates a moderate level of competition that allows only few items, n , (in this illustration $n = 2$) to be maintained in this system together.

5.1.2. Response representations

As in the model used in Section 5.1.1, the WM representation feeds into a response representation (verbal or motor). Finally, the LC is activated by a separate (perceptual) representation of the semantic probe (gray unit in Fig. 7) that decelerates exponentially towards an asymptote [$I(t) = I_L(1 - \exp(t - t_{\text{probe}}))$] and its output modulates all the inputs (including the lateral and recurrent connections) to the WM and response representations. The probe also sends a weak input, I_{probe} , to the unit that is consistent with its category (Fig. 7). The full specification of the model parameters is given in Appendix A.

Unlike the model presented in Section 4, this model is not aimed to reproduce quantitative aspects of data (see, however, Haarmann & Usher (2001)), but rather to

demonstrate the use of neuromodulation in flexible response selection.

5.2. Results and discussion

The behavior of the system in a typical trial is shown in Fig. 9 for three types of neuromodulation scenarios. The left column corresponds to a lack of neuromodulation (coupling coefficient, $c = 0$), while the middle and right columns correspond to neuromodulation with low-gain (tonic mode; middle) and high-gain (phasic-mode; right panels). The upper row corresponds to the NE response generated by the LC whereas the middle and bottom rows correspond to the perceptual and response layers, respectively. In all the simulations, four items are presented sequentially (for 500 iterations, each) and after a delay of (1600) the response cue is presented at $t = 4000$.

In the absence of neuromodulation the network parameters are fixed. We observe that before the presentation of the probe, two out of the four WM representations (corresponding to items 3 and 4) are still active. When the probe (for item no. 3) is presented, the weak input from the

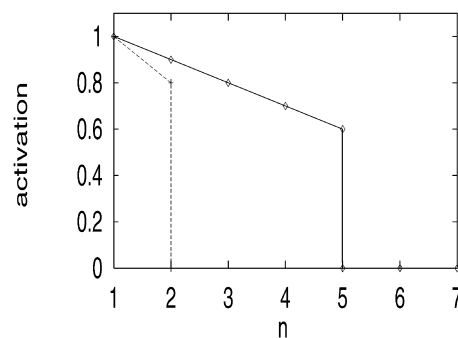


Fig. 8. Stable solutions for $\alpha = 2$ and $\beta = 0.1$, with a maximum of $n = 5$ co-active memory states (solid line), and $\alpha = 2$ and $\beta = 0.2$ with a maximum of two co-active states (dashed line).

³ The capacity, n is related to the α and β parameters via the inequality: $\alpha + \beta/[\alpha - \beta(n - 1)]^2 < 1$. Only n values that satisfy this inequality show stability (Usher & Cohen, 1999).

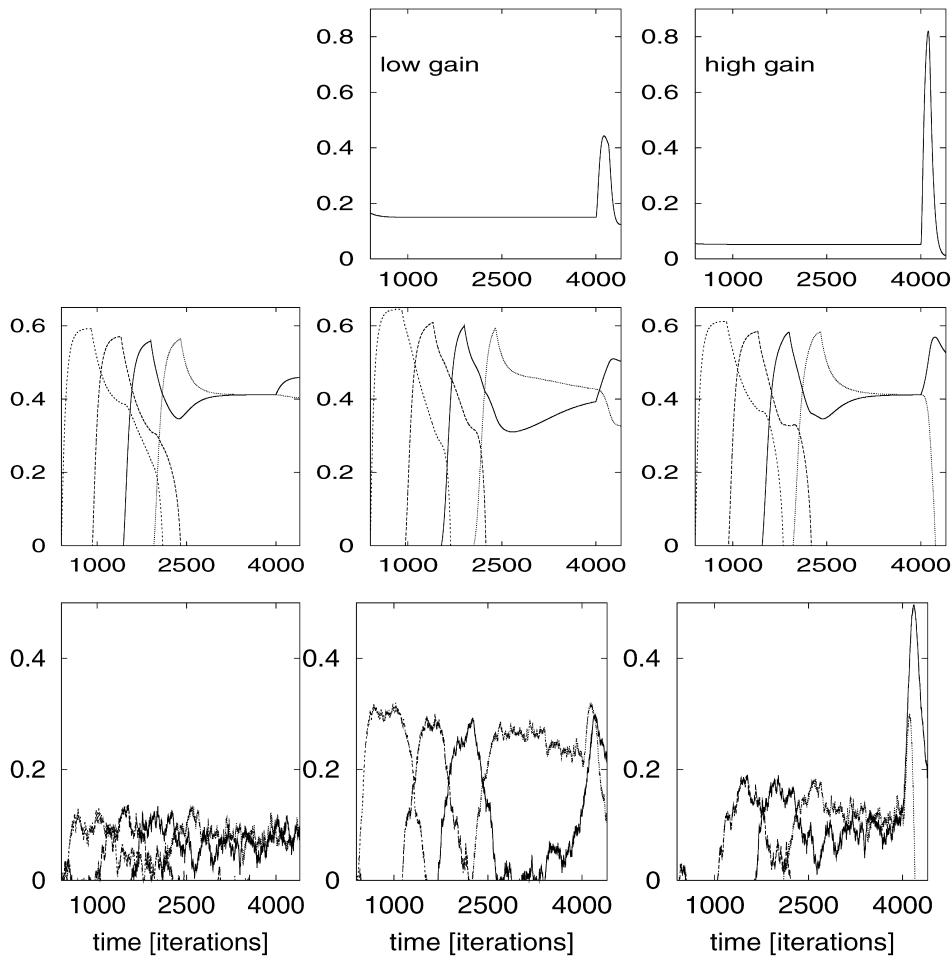


Fig. 9. Neural responses in the selection from memory model. Four items are presented sequentially for 500 iterations each, followed by a delay of 1600 iterations with no input. The probe is presented at $t = 4000$. Left: no neuromodulation ($c = 0$), Middle: low gain neuromodulation ($g = 1$, $c = 1.8$). Right: high-gain neuromodulation ($g = 3$, $c = 1.8$). Top: NE responses, Middle: firing rate responses in the WM layer ($G(m_i)$), Bottom: firing rate responses in the response layer ($G(r_i)$).

semantic probe, together with the moderate level of lateral inhibition generates a difference in the activation of the third unit (that corresponds to the probe's category) relative to the activation of the fourth unit (that corresponds to an incorrect response). This difference, however, is small, and as observed in the response activation it is not sufficient to trigger a selection between the two activated units.

With neuromodulation, the selection is enabled, but important differences appear between the high and the low gain conditions. With low gain, the tonic activation of the LC is more elevated and its phasic response is reduced, relative to the high gain (compare middle and right columns). Since NE is assumed to increase both the inhibitory and the excitatory weights, it has an effective outcome of increasing the competition between the representations (Usher & McClelland, 2001). The elevated tonic LC response in the low gain condition increases therefore the competition in the interval before the cue is given. This effectively decreases the capacity of the WM system (the system now has difficulty maintaining both units in active state) and triggers a premature selection (in the

wrong direction) in the response layer. The reduced phasic response triggered by the cue, is only marginally able to trigger the selection. As opposed to that, for the high gain neuromodulation, the tonic activity of the LC and the competition level triggered in the interval before the presentation of the cue is lower, which prevents the undesired reduction in the capacity of the WM system, and allows both of the response representations to be in a partially activated state that is optimal for choice. The enhanced phasic neuromodulation triggered by the cue, increases the competition at the relevant moment enabling a robust and correct selection.

In order to quantify these effects we ran a set of computer simulations, while varying the strength of the coupling coefficient, c , for three levels of gain, $g = 1, 1.5, 3$. The performance is measured by the relative signal strength, defined as the ratio of the correct unit activation over the total activation in the response units during the 500 iterations time interval following the response cue.

We observe that, indeed the selection quality improves with the neuromodulatory coupling (Fig. 10). More

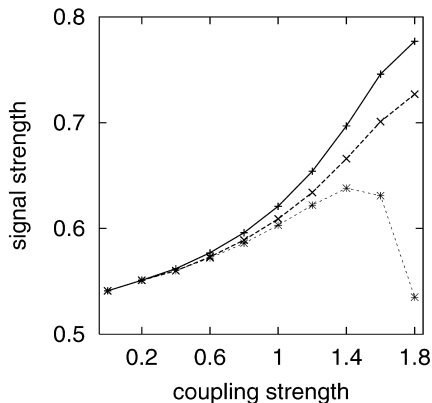


Fig. 10. The effect of neuromodulation coupling strength on the relative signal strength in the selection from memory model, for high ($g = 3$, solid with +), middle ($g = 1.5$, dashed with X) and low ($g = 1$, dashed with *) gain values.

importantly, there is an advantage for the high gain mode which is amplified at higher values of coupling. In addition, for the low gain value of $g = 1$, the effect of coupling strength is nonmonotonic. The reduction in performance at around $c = 1.4$ is due to its detrimental effect of reducing the capacity of the WM layer during the delay interval, which leads to a premature and random selection (Fig. 9, middle column).

6. General discussion

Attentional modulation of LC responses can be considered at two levels, a molar/descriptive level and a micro/mechanistic level. At the molar level, the LC modulation has been described by a gain hypothesis (Cohen & Servan-Schreiber, 1992). Accordingly, NE enhances or reduces the cortical responsivity in the high and low range, respectively. The aspect of neuromodulation explored in this paper is the dynamical modification of network parameters and input efficiency, which when triggered by online stimuli relevant to the task demand, can significantly improve the flexibility and computational power of a neural system. The NE system in the LC shows dynamic traces (phasic responses) that are phase locked to relevant stimuli and is therefore well suited to mediate this type of neuromodulation (Aston-Jones et al., 1994).

In our previous work we provided an account for the difference between the two attentional modes, corresponding to phasic/tonic responses in the LC, via changes in the level of gap-junction induced synchronization among the LC neurons (Usher et al., 1999). Here we show that, similar to the gain hypothesis of Cohen and Servan-Schreiber (1992) these two phases can be functionally reproduced by changing a single parameter that corresponds to the gain in a Wilson–Cowan circuit. Clearly, this is only a simplification of what we believe to be a more complex neurophysiological mechanism (Usher et al., 1999) and it can also be

viewed as a change in a *coherence* parameter (Gilzenrat et al., 2002).

This simplified account of neuromodulation, has allowed us to explore the effects of NE attentional modulations on a wider range of cognitive tasks. In addition to the amplification of stimulus input at relevant processing time windows, the neuromodulation affects changes in the parameters of the lateral inhibition and of the recurrent excitation of the local neural circuits. In previous work we have shown that lateral inhibition and recurrent excitation can improve the efficiency of information processing in perceptual choice by balancing the detrimental effect of neural leakage (Usher & McClelland, 2001). Flexible information processing may require, however, not only the existence of competitive and reverberatory mechanisms, but also the ability to control online their magnitudes. The task discussed in the second part of this article corresponds to a typical situation where the optimal processing strategy requires a variable degree of competition, which starts moderate (to enable memory maintenance) and ends high (to enable an effective selection).

Within this paper, we addressed the two modes of LC functioning and their computational characteristics, but not the sequential effects between trials and the processes that trigger transitions between these modes. Recently, a wide variety of sequential effects in choice and attentional tasks (e.g. slower and more accurate responses after errors), have been accounted for, by Botvinick et al. (2001), on the basis of a conflict monitoring mechanism associated with the anterior cingulate (AC) that controls parameters determining the information processing in other cortical areas. We suggest that the transient changes in the values of lateral inhibition and of the recurrent excitation, mediated by the LC, provides (in conjunction with the AC) a powerful mechanism for online control that can explain such sequential effects.

In this work we implemented the mechanism for NE neuromodulation, by assuming the enhancement of both excitatory glutaminergic and of inhibitory GABAergic synapses (Cheun & Yeh, 1992; Devilbiss & Waterhouse, 2000; Sessler et al., 1995; Waterhouse et al., 2000). Our specific implementation—an equal increase in the magnitude of the inhibitory and the excitatory weights proportional to the NE released by the LC—is only a preliminary exploration, intended to demonstrate the general feasibility of the approach and showing that neuromodulation can enhance the flexibility of online information processing. Future work should examine predictions that result from more detailed and specific effects of NE on the excitatory and inhibitory parameters of the neural circuitry.

Acknowledgments

We wish to thank Jonathan D. Cohen and Gary

Aston-Jones for insightful discussions on LC, NE and neuromodulation. EJD is a recipient of a departmental PhD studentship from the Birkbeck College.

Appendix A

The full list of model parameters used in the simulations are given below:

LC : $\lambda_x = 0.93$, $\lambda_y = 0.995$, $\lambda_{NE} = 0.98$, $a_x = 2$, $a_y = 3$, $b = 4$, $\theta_x = 1.25$, $\theta_y = 1.5$, $c = 1$ (neuromodulation coupling).

Selection from perception

Perceptual layer: $\lambda = 0.95$, $\alpha_p = 0.8$, $\beta_p = 0.22$, $\sigma_p = 0.05$ (noise SD), $I_0 = 0.2$.

Response layer: $\lambda = 0.95$, $\alpha_r = 0.2$, $\beta_r = 0.2$, $\sigma_r = 0.9$, response criterion, $z = 1$, $W^p = 1.5$ (perceptual-response weight). A response deadline of 900 iterations (400 from stimulus onset was used).

Selection from memory

Memory layer: $\lambda = 0.98$, $\alpha_m = 1.9$, $\beta_m = 0.2$, $\sigma_m = 0$, $I_i = 0.33$ (presented sequentially for 500 iterations).

Response layer: $\lambda = 0.98$, $\alpha_r = 0.3$, $\beta_r = 0.3$, $\sigma_r = 0.2$, $W^{MR} = 0.2$ (weight from memory to response layers). The probe is presented at 1600 iterations from end of last memory item, with an input to the third memory unit of $I_{\text{probe}} = 0.06$ and an input to LC, $I(t) = I_L(1 - \exp(t - t_{\text{probe}}))$, with $I_L = 1.5$ that is terminated after 200 iterations.

References

- Abbott, L. F. (1992). Firing rate models for neural populations. In O. Benhar, C. Bosio, P. Giudice, & E. Tabet (Eds.), *Neural networks: From biology to high energy physics*. Pisa: ETS Editrice.
- Ahmed, B., Anderson, J. C., Douglas, R. J., Martin, K. A. C., & Nelson, C. (1995). Comparison of current-discharge relationships of pyramidal neurons from the visual-cortex—in-vitro and in the anesthetized cat. *Journal of Neurophysiology*, *485*, 10–11.
- Ahmed, B., Anderson, J. C., Douglas, R. J., Martin, K. A. C., & Whitteridge, D. (1998). Estimates of the net excitatory currents evoked by visual stimulation of identified neurons in cat visual cortex. *Cerebral cortex*, *8*, 462–476.
- Amit, D. J., & Tsodyks, M. (1991). Quantitative study of attractor neural network retrieving at low spike rates: I substrate—Spikes, rates and neuronal gain. *Network*, *2*, 259–273.
- Anderson, J. A., Silverstein, J. W., Ritz, S. A., & Jones, R. S. (1977). Distinctive features, categorical perception and probability learning: Some applications of a neural model. *Psychological Review*, *84*, 413–451.
- Arnsten, A. F. T. (1998). Catecholamine modulation of prefrontal cortical cognitive function. *Trends in Cognitive Sciences*, *2*, 436–447.
- Aston-Jones, G., Rajkowski, J., Kubiak, P., & Alexinsky, T. (1994). Locus-Coeruleus neurons in monkey are selectively activated by attended cues in a vigilance task. *Journal of Neuroscience*, *7*, 4467–4480.
- Botvinick, M., Braver, T. S., Barch, D. M., Carter, C. S., & Cohen, J. D. (2001). Conflict monitoring and cognitive control. *Psychological Review*, *108*, 624–652.
- Cheun, J. E., & Yeh, H. H. (1992). Modulation of Gaba-A receptor-activated current by norepinephrine in cerebellar Purkinje cells. *Neuroscience*, *51*, 951–960.
- Cohen, J. D., & Servan-Schreiber, D. (1992). Context, cortex, and dopamine: A connectionist approach to behavior and biology in schizophrenia. *Psychological Review*, *99*, 45–77.
- Cowan, N. (2001). The magical number 4 in short-term memory: A reconsideration of mental storage capacity. *Behavioral and Brain Sciences*, *24*, 87–185.
- Davelaar, E. J., & Usher, M. (2002). An activation based theory of immediate memory. In J. A. Bullinaria, & W. Lowe (Eds.), *Proceedings of the Seventh Neural Computation and Psychology Workshop: Connectionist Models of Cognition and Perception* (pp. 118–131). Singapore: World Scientific.
- Devilbiss, D. M., & Waterhouse, B. D. (2000). Norepinephrine exhibits two distinct profiles of action on sensory cortical neuron responses to excitatory synaptic stimuli. *Synapse*, *37*, 273–282.
- Gilzenrat, M. S., Holmes, B. D., Rajkowski, J., Aston-Jones, G., & Cohen, J. D. (2002). Simplified dynamics in a model of noradrenergic modulation of cognitive performance. *Neural Networks*, *15*(4–5).
- Goldman-Rakic, P. S. (1992). Working memory and the mind. *Scientific American*, *267*, 111–117.
- Haarmann, H. J., & Usher, M. (2001). Maintenance of semantic information in capacity limited item short-term memory. *Journal of Psychonomic Bulletin and Review*, *8*, 568–578.
- Jagadeesh, B., Gray, C. M., & Ferster, D. (1992). Visually evoked oscillations of membrane potential in cells of cat visual cortex. *Science*, *257*, 552–555.
- Mason, A., & Larkman, A. (1990). Correlations between morphology and electro-physiology of pyramidal neurons in slices of rat visual cortex. *Journal of Neuroscience*, *10*, 1415–1428.
- McClelland, J. L. (1979). On the time relations of mental processes: An examination of systems of processes in cascade. *Psychological Review*, *86*, 287–330.
- Miller, E. K., Erickson, C. A., & Desimone, R. (1996). Neural mechanisms of visual working-memory in prefrontal cortex of the macaque. *Journal of Neuroscience*, *16*, 5154–5167.
- O'Reilly, R. C., & Munakata, Y. (2000). *Computational explorations in cognitive neuroscience. A Bradford book*. Cambridge: MIT Press.
- Sessler, F. M., Liu, W. M., Kirifides, M. L., Mouradian, R. D., Lin, R. C. S., & Waterhouse, B. D. (1995). Noradrenergic enhancement of gaba-induced resistance changes in layer-V regular spiking neurons of rat somatosensory cortex. *Brain Research*, *675*, 171–182.
- Usher, M., & Cohen, J. D. (1999). Short term memory and selection processes in a frontal-lobe model. In D. Heinke, G. W. Humphreys, & A. Olson (Eds.), *Connectionist models in cognitive neuroscience* (pp. 78–91). Berlin: Springer, www.psyc.bbkc.ac.uk/staff/mu.html.
- Usher, M., & McClelland, J. L. (2001). On the time course of perceptual choice: A model based on principles of neural computation. *Psychological Review*, *108*, 550–592.
- Usher, M., Cohen, J. D., Haarmann, H. J., & Horn, D. (2001). Neural mechanism for the magical number 4: Competitive interactions and non-linear oscillations. *Behavioral and Brain Sciences*, *24*, 151.
- Usher, M., Cohen, J. D., Servan-Schreiber, D., Rajkowski, J., & Aston-Jones, G. (1999). The role of locus coeruleus in the regulation of cognitive performance. *Science*, *283*, 549–554.
- Waterhouse, B. D., Mouradian, R., Sessler, F. M., & Lin, R. C. S. (2000). Differential modulatory effects of norepinephrine on synaptically driven responses of layer V barrel field cortical neurons. *Brain Research*, *868*, 39–47.
- Wilson, H., & Cowan, J. (1972). Excitatory and inhibitory interactions in localized populations of model neurons. *Biological Cybernetics*, *12*, 1–24.